Journal of Materials Chemistry C

Controlled aqueous synthesis of ultra-long copper nanowires for stretchable transparent conducting electrode

Journal:	*Journal of Materials Chemistry C*
Manuscript ID	TC-ART-11-2015-003614.R1
Article Type:	Paper
Date Submitted by the Author:	28-Dec-2015

Complete List of Authors:	Hwang, Cha Hwan; Chung-Ang University, Department of Chemistry Choi, Byung Doo; Chung-Ang University, Department of Chemistry An, Jihyun; Seoul National University, Chemistry Education Kim, Kwanpyo; Ulsan National Institute of Science and Technology (UNIST), Department of Physics Jung, Soon-Won; ETRI, Baeg, Kang-Jun; Pukyong National University, Department of Graphic Arts Information Engineering Kim, Myung-Gil; Chung-Ang University, Department of Chemistry Ok, Kang Min; Chung-Ang University, Chemistry Hong, Jongin; Chung-Ang University, Chemistry

Journal of Materials Chemistry C

PAPER

Controlled aqueous synthesis of ultra-long copper nanowires for stretchable transparent conducting electrode

Received 00th January 20xx,
Accepted 00th January 20xx

DOI: 10.1039/x0xx00000x

www.rsc.org/

Cha Hwan Hwang,[a] Jihyun An,[b] Byung Doo Choi,[a] Kwanpyo Kim,[c] Soon-Won Jung,[d] Kang-Jun Baeg,[e] Myung-Gil Kim,[a]* Kang Min Ok[a]* and Jongin Hong[a]*

The environmentally benign synthesis of ultra-long copper nanowires with successful controls of diameter and length for stretchable transparent conducting electrodes (TCEs) is reported. The ultra-long copper nanowires (CuNWs) with an average length of 92.5 μm (maximum length up to 260 μm) and an average diameter of 47 nm were synthesized using environmentally friendly water-alcohol mixtures and L-ascorbic acid as a reducing agent. A facile removal of insulating surface layers, such as organic capping molecules and copper oxide/hydroxide, by short-chain organic acid treatment allowed for low contact resistance between the CuNWs without post-reductive treatment at elevated temperature. The CuNWs were directly spray-coated on glass or polydimethylsiloxane (PDMS) with low pocessing temerapture at 130 °C. The CuNWs TCE on glass substrate exhibited low sheet resistance of 23.1 Ohm/sq and high optical transmittance of 84.1 % at 550 nm. Furthermore, the CuNWs were directly spray-coated on a stretchable PDMS showed low sheet resistance of 4.1 Ohm/sq and high optical transmittance of 70 % at 550 nm.

1. Introduction

The transparent conducting electrode (TCE) is one of the essential building blocks for diverse optoelectronic devices including flat panel display (FPD),[1, 2] thin-film solar cell,[3, 4] touch screen panel (TSP)[5-7] and smart window.[8-10] The indium tin oxide (ITO) has been successfully used as an industrial standard TCE with high optical transmittance (T_{550}) of ~90 % at 550 nm and low sheet resistance (R_s) of 5~40 Ohm/sq.[11-13] Unfortunately, typical ITO films are inappropriate for next-generation optoelectronic applications, such as flexible displays, rollable solar cells, and wearable electronic devices, due to high cost of indium, expensive vacuum processes, and mechanical brittleness.[14-17] Over the last decade there has been robust research interest in low-cost alternative TCE materials with improved optoelectronic properties and exceptional mechanical stabilities. The intensive work on conducting polymers (e.g. PEDOT:PSS), carbon materials (e.g. carbon nanotubes and graphene),[18-27] metal oxides (e.g. AZO, ZITO, CdO:In and FTO),[28-35] and metal nanostructures (e.g. nanogrids and nanowire networks)[36-40] has been reported. Among them, the metal nanowire networks have attracted much attention because they can be cost-effectively processed by coating a nanowire solution on a substrate. Importantly, a facile and scalable synthesis of metal nanowires and their chemical inertness render the metal nanowire networks as emerging TCEs. Additionally, networks of nanowires with a high aspect ratio can maintain their continuous network structure under mechanical stresses. To date, the nanowire syntheses of noble metals (e.g. Au, Ag, Pt and Pd) and base metals (e.g. Ni and Cu) and fabrication of their networks have been demonstrated. In particular, copper is 1,000 times more abundant and 100 times cheaper than silver.[14] Moreover, the electrical resistivity of copper (1.68×10^{-6} Ohm·cm) is similar to that of silver (1.59×10^{-6} Ohm·cm) and much lower than that of Ni (6.93×10^{-6} Ohm·cm).[40] Therefore, the development of copper nanowires (CuNWs) and their networks is crucial for preparing low-cost transparent flexible/stretchable electrodes.

Recently, several studies on CuNW TCEs could achieve equivalent or even superior optoelectronic performance to the conventional ITO electrode, with exceptional mechanical stability. Lu *et al*. reported the CuNW TCE, which has R_s = 35 Ohm/sq and T_{550} = 85%.[41]. With thinner CuNWs, Peng *et al*. showed CuNW TCE of R_s = 51.5 Ohm/sq and T_{550} = 93.1%.[42] More recently, Wiley *et al*. reported CuNW TCE with T_{550} > 95% and R_s < 100 Ohm/sq.[43] The aforementioned CuNWs can be synthesized by using various methods, such as hydrothermal reaction and hydrazine reduction method. For example, high

[a] Department of Chemistry, Chung-Ang University, Seoul 156-756, Republic of Korea. *E-mail: myunggil@cau.ac.kr; kmok@cau.ac.kr; hongj@cau.ac.kr; Fax +82 2-825-4736
[b] Department of Chemistry Education, Seoul National University, Seoul, 151-748, Republic of Korea.
[c] Department of Physics, Ulsan National Institute of Science and Technology (UNIST), Ulsan 689-798, Republic of Korea.
[d] Convergence Components and Materials Research Laboratory, Electronics and Telecommunications Research Institute (ETRI), Daejeon 305-700, Republic of Korea.
[e] Department of Graphic Arts Information Engineering, Pukyong National University, Busan 608-739, Republic of Korea.

Electronic Supplementary Information (ESI) available: [The length and diameter analysis graph of copper nanowires, the field-emission scanning electron microscope images, and the x-ray photoelectron spectroscopy spectra.]. See DOI: 10.1039/b000000x/

aspect ratio CuNWs from the hydrazine reduction method exhibited ITO comparable optoelectronic performance. However, the use of hydrazine makes the reaction inappropriate for industrial applications due to significant environmental issues and health problems. Meanwhile, very long CuNWs can be synthesized by hydrothermal reactions from an alkylamine-copper complex. Unfortunately, because this method produces highly agglomerated or bundled CuNWs, only small amount of the nanowires can be used for coating them on the substrate after filtration.[41] Furthermore, these methods are difficult to control the diameter and length of the nanowires.

Generally, the lack of facile control on copper nanowire morphology is observed in most of the synthetic routes. Since there are numerous subtle synthesis parameters, such as initiator condition, precursor concentration, temperature, and reaction time, it is not easy to regulate the formation of particulates as well as their diameter and length. Moreover, high temperature annealing in an reductive environment is typically required to remove surfactants and surface oxide.[41, 42] These make the nanowires not amenable to flexible or stretchable substrates.

In this study, we developed a rational method to control the diameter and length of CuNWs at the low reaction temperature using an unsaturated alkyl amine and environmentally friendly ascorbic acid as a ligand and a reducing agent, respectively. The spray-coated CuNWs TCE on glass substrate exhibited low sheet resistance of 23.1 Ohm/sq and high optical transmittance of 84.1 % at 550 nm. Furthermore, the in-situ replacement of the long alkyl amine on the nanowires' surface with short propionic acid allowed for a direct fabrication of the CuNW TCE on the thermally labile stretchable polydimethylsiloxane (PDMS) substrate with excellent high optical transmittance (T_{550} = 70%) and low sheet resistance (R_s = 4.1 ohm/sq).

2. Results and discussion

To achieve the scalable fabrication of copper nanowire networks on thermally labile flexible or stretchable substrates, we developed a new method which involves a controlled copper nanowire synthesis, solution phase surfactant exchange process at room temperature and a large area compatible direct spray-coating method, as summarized in Fig. 1. The rational synthetic control using temperature and the co-solvent system in Fig. 1a allowed for controlling the nanowire diameters. As shown in Fig. 1b, the *in-situ* ligand exchange with propionic acid allowed the facile removal of insulating surface ligand. Moreover, the surface oxide etching with acetic acid resulted low contact resitance between CuNWs. Overall, CuNWs TCE can be directly spray-coated at low temperature without the high temperature reductive post-annealing process.

Fig. 2 shows the effect of aging temperature control, using oleylamine as a capping ligand and ascorbic acid as a reducing agent in distilled water (DW). The synthesized nanowires have average diameters of 297 nm at 55 ^{o}C (Fig. 2a), 265 nm at 65 ^{o}C (Fig. 2b), 166 nm at 75 ^{o}C (Fig. 2c), and 110 nm at 85 ^{o}C (Fig. 2d). When temperature increased from 55 ^{o}C to 85 ^{o}C, the significant decrease in

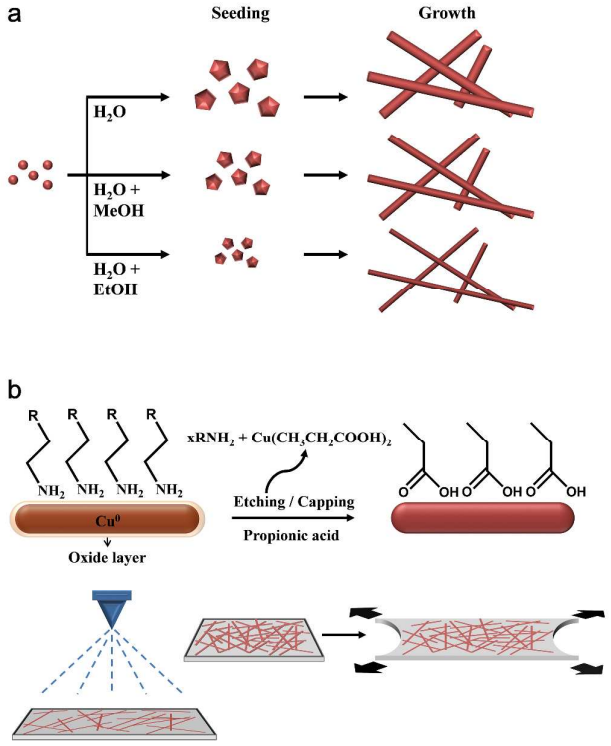

Figure 1. Schematic diagram of copper nanowire morphology control and annealing free fabrication. (a) Controlled synthesis of copper nanowire using co-solvents. (b) Low temperature fabrication of copper nanowire transparent conducting electrode with short ligand exchange and spray coating.

nanowire diameter and its variation was observed (Fig. 2 and Fig. S1). As reported in ref. [44], the growth of copper nanowire requires an initial formation of twinned crystalline metal seeds. The high reaction temperature induces the fast nucleation of crystalline copper seeds of a smaller size and a subsequent initiation of the anisotropic nanowire

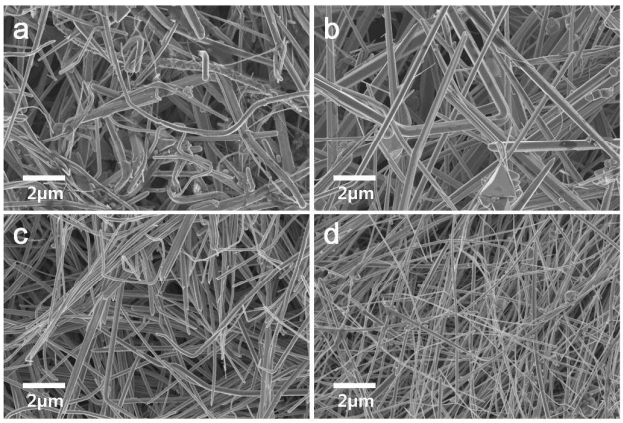

Figure 2. Field emission scanning electron microscopy (FESEM) images of copper nanowires synthesized at (a) 55 ^{o}C, (b) 65 ^{o}C, (c) 75 ^{o}C, (d) 85 ^{o}C in distilled water.

growth. The faster longitudinal growth as opposed to the isotropic growth of copper seeds at high temperature allows for a formation of nanowires with smaller diameters. Since the minimized time of the isotropic seed growth suppresses the copper seed diameter variation, the higher temperature provides well defined nanowire diameter (Fig. S1 and Table S1). The X-ray diffraction (XRD) patterns in Fig. 3a represent the as-synthesized CuNWs at 85 °C in DW. Each peak corresponds to (111), (200) and (220) planes in face-centered cubic phase respectively without significant amount of oxidized impurities, such as Cu_2O or CuO. The representative transmission electron microscopy (TEM) image and electron diffraction pattern of the synthesized CuNW in Fig. 3b shows that copper nanowires of 150 nm diameters were grown in [011] direction without any particulates. With the preferred absorption of primary amines, such as hexadecylamine, on (100) plane, copper could be grown as a long wire when the copper ion was slowly supplied because of the poor solubility of the copper complexes in aqueous solution. [2-11] and [100] zones in the electron diffraction patterns which are marked in green and yellow respectively (Fig. 3b), confirm a typical five-fold twinned structure of Cu nanowire.[45-48]

Further control on copper nanowire morphology was achieved with the water-alcohol co-solvent. Fig. 4 shows the as-synthesized copper nanowires using different alcohol co-solvents, such as methanol, ethanol, *n*-propanol and *n*-butanol under 85 °C. As the hydrophobicity of alcohol increases, the nanowire mean diameter is decreased from 110 nm (pure DW) to 47 nm (DW with *n*-propanol). The decrease of the diameter was attributed to the solubility increase of the metal complex in co-solvent system. The water-miscible low carbon number alcohols enhanced the solubility of hydrophobic molecule in water. Since the copper-oleylamine complex from the reactant mixture has long hydrophobic alkyl chains, the initial metal source has a higher solubility in DW-alcohol co-solvent system than pure water. The SEM images in Fig. 4 show that increase of the carbon number in the alcohol resulted thinner nanowires of 78 nm, 64 nm and 47 nm in methanol, ethanol and *n*-propanol, respectively. The higher concentration of the copper complex, resulting from the higher solubility in alcohols, induced more uniform seed particle formation and rapid longitudal (111) plane nanowire growth. As shown in Figs. S2-3 and Table S2, the short initial seed formation time, due to the higher concentration of the copper complex, suppressed the Ostwald ripening process among metal seeds with minimizing inhomogeneous size of the seeds and diameter variation of the nanowires. However,

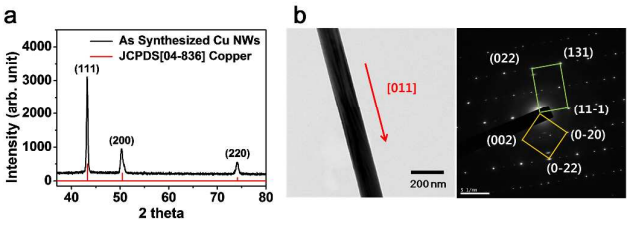

Figure 3. Characterization of copper nanowire (CuNW) synthesized at 85 °C in water. (a) X-ray diffraction pattern of CuNW. (b) TEM image and electron diffraction pattern of five-fold twinned CuNW.

the further increase of hydrophobicity in *n*-butanol resulted in particles rather than nanowire formation. Unlike the completely water-miscible small alcohols, the heterogeneous microemulsion, due to low water solubility of butanol (0.11 mol/100g at 20 °C), hindered anisotropic nanowire growth and resulted in shapeless particles, as shown in Fig. 4d. The effect of co-solvent hydrophobicity was further investigated by solvent-ratio control. When a methanol-water mixture was used, the increase of methanol ratio from 10 vol% to 15 vol% yielded small diameter nanowires with some nanoparticle impurities (Fig. S4 a-b). In the ethanol co-solvent system, the increase of ethanol from 10 vol% to 15 vol% afforded the nanowires with smaller diameter and higher particle content (Figs. S4 c-d). As shown in Figs. S4 e-f, the increased hydrophobicity of *n*-propanol from 10 vol% to 15 vol% resulted mostly submicron particles. Although the increased hydrophobicity resulted in thinner nanowires, the higher ratio of *n*-propanol or *n*-butanol in co-solvents did not afford proper anisotropic nanowire growth. Because the large difference in hydrophobicity is required for stable micelle formation and anisotropic nanowire growth, the higher water content is necessary. Ultimately, the optimized ratio of hydrophobic alcohol and water is critical for pure nanowire growth with desired morphology.

To achieve a high quality TCE, the copper nanowires should be well dispersed in a solvent. In general, the removal of the capping ligand intertwines copper nanowires and destabilizes the dispersion,[49] which makes the nanowires inappropriate for high throughput processes, such as spray-coating, bar-coating, and roll-to-roll (R2R) printing. Although few reports demonstrated a stable dispersion with high molecular weight polyvinylpyrrolidone (PVP) surfactant,[41, 49] the removal of capping ligands at high temperature makes the dispersion incompatible with thermally labile flexible or stretchable substrates. The contradictory aspect of stable dispersion and easy removal of capping ligands can be accomplished using a short-chain surfactant. In our experiment, after the nanowire growth, the solution was centrifuged and the supernatant was decanted. The precipitated nanowires were washed with 5 wt% propionic acid in toluene, and

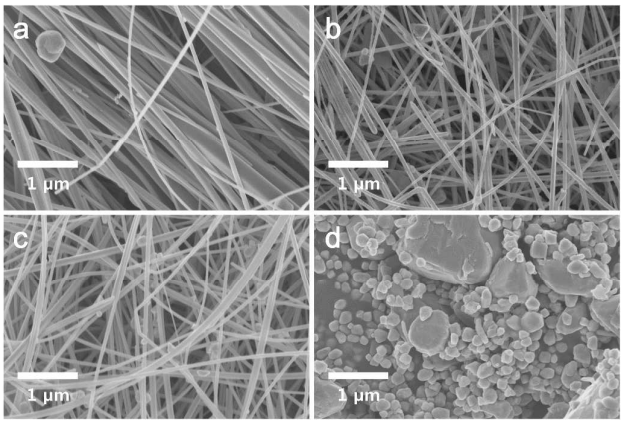

Figure 4. FESEM images of copper nanowires synthesized with different co-solvents at 85 °C. (a) 1ml of methanol, (b) 1ml of ethanol, (c) 1ml of n-propanol, and (d) 1ml of n-butanol were used as co-solvent with 18 ml distilled water.

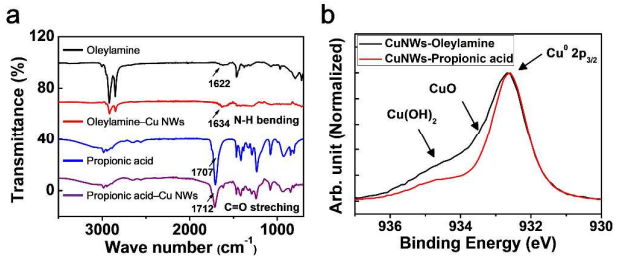

Figure 5. (a) FT-IR spectra and (b) Cu 2*p* XPS spectra of oleylamine capped CuNWs and ligand exchanged CuNWs with propionic acid.

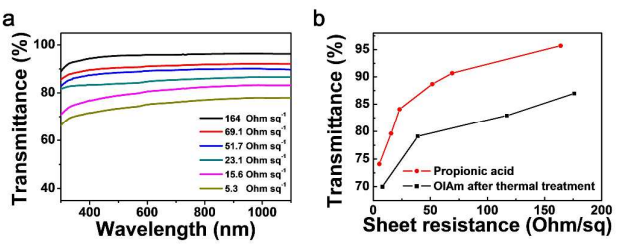

Figure 6. Optoelectronic characterization of CuNWs TCE. (a) Transmittance of CuNWs TCE on top of glass in the visible-light range. (b) Sheet resistance vs. transmittance plots of CuNWs with different surface ligand.

dispersed in isopropanol. As shown in the infrared spectrum of Fig. 5a, the oleylamine is completely exchanged with propionic acid. As shown in the infrared spectrum of Fig. 5a, the oleylamine is completely exchanged with propionic acid. The N-H bending peaks at

1634 cm^{-1} disappeared and a new C=O stretching at 1712 cm^{-1} emerged after ligand exchange. As confirmed with Cu 2*p* XPS data in

Fig. 5b, the significant suppression of Cu-O and Cu-OH related XPS peak shows that the organic acid etched oxide layer on the Cu nanowire.

Our stable low temperature processable copper nanowire dispersion could be easily applied on flexible or stretchable substrates with high throughput continuous processing methods. Fig. 6a shows transmittance and corresponding sheet resistance of the spray-coated copper nanowires TCE on a glass substrate. The corresponding morphology of CuNWs TCEs are shown in Fig S5. Using the glass substrate, excellent optical transmittance (T_{550}) over 95 % and 91 % at 550 nm were achieved with sheet resistance (R_s) of 164 ohm/sq and 69 Ohm/sq, respectively, which were comparable to commercially available ITO electrodes (R_s ~ 40 Ohm/sq and T_{550} ~ 90 %)[11] The atomic force microscopy (AFM) image of CuNWs TCE in Figs. S6 reveals that the height of stacked nanowire junction is around 80 nm. The rough surface of CuNWs TCE could be improved by additional smoothing layers or a mechanical pressing process.[50-52] Unlike most of the previous reports, the as-fabricated copper nanowires TCE shows a decent performance without post-annealing process for surfactant removal and/or nanowire junction welding. As confirmed with bulk samples in Fig. 5 and Fig. S7, the ligand exchange of oleylamine with propionic acid is crucial for the low temperature removal of surfactants. The as-prepared oleylamine capped CuNWs showed typically immeasurable high resistance. Although the high temperature annealing at 300 °C removed oleylamine on the Cu nanowire and improved R_s to ~175 Ohm/sq with T_{550} = 86%, the high temperature processing is inappropriate for the direct fabrication of CuNWs TCE on thermally labile flexible or stretchable substrates. As shown in Fig. 6b, the ligand exchange of the CuNWs with propionic acid significantly improved the sheet resistance of CuNWs TCE by removing the insulating long alkyl chains.

The ligand exchanged CuNWs even showed superior electrical performance to high temperature annealed NWs. In addition to the facile ligand removal, the significant electrical performance improvement is attributed to the removal of insulating surface oxide. resulted the surface oxide, the addition of acetice acid before spray coating ensure the oxide removal. The contact enhancement between As mentioned above, the substantial suppression of the Cu-O and Cu-OH related XPS peaks in Fig. 5b confirms the improved electrical connection between NWs. Since the long term storage of CuNWs nanowires allows low nanowire junction resistance of the as-fabricated TCE on a thermally labile substrate.

The long term stability of CuNWs has been a significant obstacle for the realization of CuNWs TCE. The storage of CuNWs TCE under ambient air resulted in the surface oxidation of CuNWs and the degradation of electrical performance. Using the accelerated test condition of 60 °C under ambient air, Fig. S8 shows the sheet resistance degradation of as-fabricated CuNWs TCE with R_s values of 30-40 ohm/sq. The oxidation of CuNWs surface increased the junction resistance between CuNWs. After 3 days at 60 °C under ambient air, the CuNWs TCE showed a significant increase of R_s values up to 4-5 times of initial values or sample failure, comparable to typically reported CuNWs TCE.[53-55] The sample failure time shows sample-to-sample variation of 3 to 6 days. Fortunately, the long term storage of CuNWs TCE can be significantly improved by the surface coating of Ni and the embedding of CuNWs into elastomer matrix.[55, 56]

Finally the low temperature processable CuNWs dispersion was successfully applied on thermally labile substrates. Fig. 7a shows the photograph of the stretchable spray-coated CuNWs TCE on the PDMS substrates. The stretchable TCE initially exhibited sheet resistance of 4.1 Ohm/sq with 70% optical transmittance at 550 nm. The CuNWs TCE displayed a resistance increase about nine fold after 30% strain. A further strain of over 50% significantly destroyed electrical connections between the nanowires and rapidly increased R_s over 100 times. With the repeated strain cycle of 20% on CuNWs TCE, the resistivity increase was stabilized after 20 cycles. At the initial cycle, the CuNW networks were destroyed with residual conductivity from mechanically robust connection points. Fig. S9 clearly shows the rupture of CuNWs connection and the aggregated bundle formation under mechanical strain. Our stretchable TCE shows resistivity increase of R/R_0 ~ 2.1 at 10 % strain, comparable to typical reported stretchable CuNWs TCE.[57] The the weak adhesion and low density of CuNWs on PDMS substrate could degrade the stretchability of metal NWs TCE. Previously, the plasmonic welding of metal NWs junction,

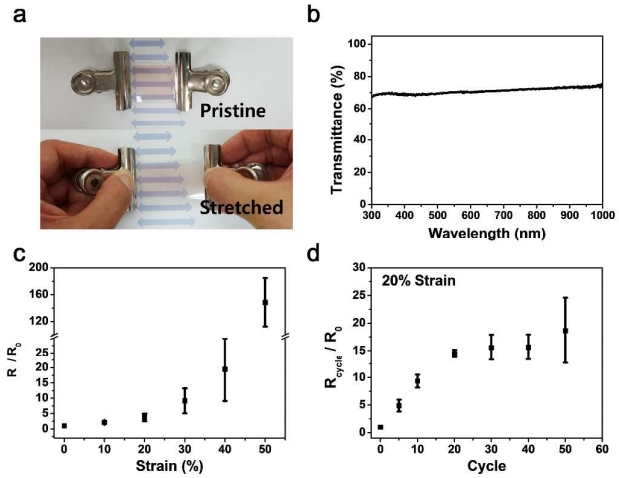

Figure 7. Stretchable CuNWs transparent conducting electrode with PDMS substrate. (a) Photograph of stretchable CuNWs TCE on PDMS substrate. (b) Transmittance of CuNWs TCE on top of PDMS in the visible-light range. (c) Relative sheet resistance change of the 4.17 ohm/sq electrode during first stretching cycle. (d) Relative resistance change of 4.1 ohm electrode during repeated 20% strain.

the embedded NWs in elastomeric matrix, and direct deposition of metal NWs on prestrained substrate improved electrical stability of metal NWs TCE under mechanical strain.[55, 58-60] The further study on optimized substrates and deposition conditions could enhance the mechanical stability of CuNWs TCE.

3. Conclusions

We have successfully demonstrated the low temperature fabrication of the CuNWs TCEon thermally labile substrates, using the environmental-friendly rational synthetic route and the facile annealing free ligand removal method. The newly developed synthetic route for size-controlled CuNWs used nontoxic solvents and a reducing agent; water/alcohol mixture and ascorbic acid, respectively. The successful control of the diameter and length was achieved down to 47 nm and up to 260 μm through the solubility control of the copper complex in the n-propyl alcohol based co-solvent system. The insulating and non-volatile oleylamine ligand was exchanged with easily removable propionic acid. Combining the acetic acid additive and propionic acid ligand, the copper nanowire dispersion can be spray-coated on the glass and PDMS at the low temperature of 130 ^{o}C. The low sheet resistance and high transmittance of the spray-coated CuNWs TCE show that the CuNWs TCE can be industrially implemented for high performance low cost flexible/stretchable electronics.

4. Experimental section

Reagents

Copper(II) chloride dihydrate ($CuCl_2 \cdot 2H_2O$, 99%), L-ascorbic acid (99%), oleylamine (70%) were purchased from Sigma-Aldrich. All reagents were used without further purification.

Synthesis of copper nanowires

Copper chloride dehydrate (0.2M) and L-ascorbic acid (0.2M) were dissolved in distilled water (DW). After diluting 1 mL copper chloride solution with 18 mL DW, 0.12 mL of oleylamine was added to the solution. Then the mixed solution was sonicated with a horn type sonicator for 30 s at 150 W to prepare the white-blue emulsion. The 1 mL of L-ascorbic acid solution was added to the copper complex emulsion. The solution was aged at 55-85 ^{o}C for 12 h.

Diameter controlled copper nanowires were synthesized with the similar method. Reagent solutions were added to the methanol, ethanol or *n*-propanol based alcohol-DW co-solvents.

After cooling down to room temperature, the supernatant was decanted to collect nanowire precipitates. The nanowires were washed with isopropanol (IPA) for 3 times.

All the reported materials have been deposited to Noncentrosymmetric Materials Bank (http://ncsmb.knrrc.or.kr).

Surface ligand exchange

20 mL of 5 wt% propionic acid in toluene solution was added to the washed nanowire precipitates. After dispersing the precipitates by shaking, the nanowires were centrifuged at 2000 rpm for 3 min. The supernatant was decanted. The exchange procedure was repeated for 2 times. Finally, ligand exchanged nanowires were washed with pure IPA for 3 times.

Fabrication of Cu nanowires transparent conducting electrode

A network of CuNWs was prepared using air brush (ZECO) on glass or PDMS substrates. The CuNWs dispersion was spray-coated on the desired substrate at 130 ^{o}C with air pressure of 1 atm. The transparency of electrode was controlled with varying the spraying time. In case of oleylamine capped CuNWs transparent electrode, the electrode was additionally heated at 300 ^{o}C in forming gas (5% H_2 and 95% Ar) filled tube furnace for 1 hour. To fabricate annealing-free CuNWs TCE, 1 mL of acetic acid was added to the ligand exchanged nanowire dispersion.

Characterization of Cu nanowires network

X-ray diffraction pattern was obtained using D8-Advance (Bruker-AXS, Germany) with a step size of 0.02^{o} at scan rate of 0.2 s/step. The atomic force microscopy images with non-contact mode was obtained with XE-120-AFM (Park Systems, Korea). Al-coated non-contact tips (Nanosensors, PPP-NCHR, Switzerland, force constant (k) = 42 N/m, resonance frequency = 330 kHz) were used for the atomic force microscopy imaging, and the scan rate was 1.0 Hz. Field emission scanning electron microscopy (FESEM) images were obtained at 5 kV accelerating voltage with SIGMA (Carl Zeiss, Germany). Transmission electron microscopy (TEM) images and electron diffraction (ED) pattern were acquired at 200 kV using a JEM-4010 (JEOL, Japan) on carbon-coated gold grid. The optical spectra were measured with V-730 UV-Vis spectrometer (JASCO, USA). FT-IR spectroscopy was carried out using an attenuated total reflection mode Nicolet iS10 FT-IR spectrometer (Thermo Scientific, USA). X-ray photoemission spectroscopy (XPS) spectra were obtained using Al K-alpha

(Thermo Scientific, USA). The sheet resistance was measured with four point probe station (MST-4000A, MS TECH) and semiconductor analyser (HP 4145B). The resistance change with stretching was measured using manually adjustable homemade sample holder with two point probe and semiconductor analyser (HP 4145B).

Acknowledgements

This work was supported by the National Research Foundation of Korea (NRF) grant funded by the Korea government (MSIP) (No. 2014R1A1A1036176 and 2014M3A9B8023478).

References

1. L. C. Gontijo, A. G. Cunha and P. A. P. Nascente, *Mater. Sci. Eng., B*, 2012, **177**, 1783-1787.
2. R. Gupta, K. D. M. Rao, K. Srivastava, A. Kumar, S. Kiruthika and G. U. Kulkarni, *ACS Appl. Mater. Interfaces*, 2014, **6**, 13688-13696.
3. S. Calnan and A. N. Tiwari, *Thin Solid Films*, 2010, **518**, 1839-1849.
4. K. Schulze, B. Maennig, K. Leo, Y. Tomita, C. May, J. Huepkes, E. Brier, E. Reinold and P. Baeuerle, *Appl. Phys. Lett.*, 2007, **91**.
5. M. H. Ahn, E. S. Cho and S. J. Kwon, *Appl. Surf. Sci.*, 2011, **258**, 1242-1248.
6. S. F. Tseng, W. T. Hsiao, K. C. Huang, D. Chiang, M. F. Chen and C. P. Chou, *Appl. Surf. Sci.*, 2010, **257**, 1487-1494.
7. H. Wu, L. Hu, T. Carney, Z. Ruan, D. Kong, Z. Yu, Y. Yao, J. J. Cha, J. Zhu, S. Fan and Y. Cui, *J. Am. Chem. Soc.*, 2011, **133**, 27-29.
8. A. Azens and C. G. Granqvist, *J. Solid State Electrochem.*, 2003, **7**, 64-68.
9. C. M. Lampert, *Sol. Energy Mater. Sol. Cells*, 2003, **76**, 489-499.
10. K. Tajima, Y. Yamada, S. Bao, M. Okada and K. Yoshimura, *Appl. Phys. Lett.*, 2007, **91**, 051908.
11. D. H. Wang, A. K. K. Kyaw, V. Gupta, G. C. Bazan and A. J. Heeger, *Adv. Energy Mater.*, 2013, **3**, 1161-1165.
12. H. Kim, J. S. Horwitz, G. Kushto, A. Pique, Z. H. Kafafi, C. M. Gilmore and D. B. Chrisey, *J. Appl. Phys.*, 2000, **88**, 6021-6025.
13. C. C. Wu, C. I. Wu, J. C. Sturm and A. Kahn, *Appl. Phys. Lett.*, 1997, **70**, 1348-1350.
14. A. R. Rathmell, S. M. Bergin, Y. L. Hua, Z. Y. Li and B. J. Wiley, *Adv. Mater.*, 2010, **22**, 3558-3563.
15. Z. Chen, B. Cotterell, W. Wang, E. Guenther and S. J. Chua, *Thin Solid Films*, 2001, **394**, 202-206.
16. Y. F. Lan, W. C. Peng, Y. H. Lo and J. L. He, *Org. Electron.*, 2010, **11**, 670-676.
17. K. A. Sierros, N. J. Morris, K. Ramji and D. R. Cairns, *Thin Solid Films*, 2009, **517**, 2590-2595.
18. H. Chang, G. Wang, A. Yang, X. Tao, X. Liu, Y. Shen and Z. Zheng, *Adv. Funct. Mater.*, 2010, **20**, 2893-2902.
19. B. Dan, G. C. Irvin and M. Pasquali, *ACS Nano*, 2009, **3**, 835-843.
20. S. De, P. E. Lyons, S. Sorel, E. M. Doherty, P. J. King, W. J. Blau, P. N. Nirmalraj, J. J. Boland, V. Scardaci, J. Joimel and J. N. Coleman, *ACS Nano*, 2009, **3**, 714-720.
21. Y. H. Ha, N. Nikolov, S. K. Pollack, J. Mastrangelo, B. D. Martin and R. Shashidhar, *Adv. Funct. Mater.*, 2004, **14**, 615-622.
22. D. S. Hecht, L. Hu and G. Irvin, *Adv. Mater.*, 2011, **23**, 1482-1513.
23. Y. H. Kim, C. Sachse, M. L. Machala, C. May, L. Mueller-Meskamp and K. Leo, *Adv. Funct. Mater.*, 2011, **21**, 1076-1081.
24. J. M. Schnorr and T. M. Swager, *Chem. Mater.*, 2011, **23**, 646-657.
25. M. Vosgueritchian, D. J. Lipomi and Z. Bao, *Adv. Funct. Mater.*, 2012, **22**, 421-428.
26. J. Wu, M. Agrawal, H. A. Becerril, Z. Bao, Z. Liu, Y. Chen and P. Peumans, *ACS Nano*, 2010, **4**, 43-48.
27. Z. Yin, S. Sun, T. Salim, S. Wu, X. Huang, Q. He, Y. M. Lam and H. Zhang, *ACS Nano*, 2010, **4**, 5263-5268.
28. X. Jiang, F. L. Wong, M. K. Fung and S. T. Lee, *Appl. Phys. Lett.*, 2003, **83**, 1875-1877.
29. H. W. Lee, S. P. Lau, Y. G. Wang, K. Y. Tse, H. H. Hng and B. K. Tay, *J. Cryst. Growth*, 2004, **268**, 596-601.
30. T. Minami, T. Yamamoto, Y. Toda and T. Miyata, *Thin Solid Films*, 2000, **373**, 189-194.
31. M. V, B. Teixeira, E. Fortunato, R. C. C. Monteiro and P. Vilarinho, *Surf. Coat. Technol.*, 2004, **180**, 659-662.
32. A. Nadarajah, M. E. Carnes, M. G. Kast, D. W. Johnson and S. W. Boettcher, *Chem. Mater.*, 2013, **25**, 4080-4087.
33. L. L. Pan, K. K. Meng, G. Y. Li, H. M. Sun and J. S. Lian, *RSC Adv.*, 2014, **4**, 52451-52460.
34. Y. K. Zhu, R. J. Mendelsberg, J. Q. Zhu, J. C. Han and A. Anders, *Appl. Surf. Sci.*, 2013, **265**, 738-744.
35. J. Z. Song, S. A. Kulinich, J. H. Li, Y. L. Liu and H. B. Zeng, *Angew Chem Int Edit*, 2015, **54**, 462-466.
36. D. Y. Choi, H. W. Kang, H. J. Sung and S. S. Kim, *Nanoscale*, 2013, **5**, 977-983.
37. J. Jiu, T. Araki, J. Wang, M. Nogi, T. Sugahara, S. Nagao, H. Koga, K. Suganuma, E. Nakazawa, M. Hara, H. Uchida and K. Shinozaki, *J. Mater. Chem. A*, 2014, **2**, 6326.
38. H.-J. Kim, S.-H. Lee, J. Lee, E.-S. Lee, J.-H. Choi, J.-H. Jung, J.-Y. Jung and D.-G. Choi, *Small*, 2014, **10**, 3767-3774.
39. T. Kim, A. Canlier, G. H. Kim, J. Choi, M. Park and S. M. Han, *ACS Appl. Mater. Interfaces*, 2013, **5**, 788-794.
40. J. Usagawa, S. S. Pandey, Y. Ogomi, S. Noguchi, Y. Yamaguchi and S. Hayase, *Prog. Photovolt.*, 2013, **21**, 517-524.
41. D. Zhang, R. Wang, M. Wen, D. Weng, X. Cui, J. Sun, H. Li and Y. Lu, *J. Am. Chem. Soc.*, 2012, **134**, 14283-14286.
42. H. Guo, N. Lin, Y. Chen, Z. Wang, Q. Xie, T. Zheng, N. Gao, S. Li, J. Kang, D. Cai and D. L. Peng, *Sci Rep*, 2013, **3**, 2323.
43. I. E. Stewart, A. R. Rathmell, L. Yan, S. Ye, P. F. Flowers, W. You and B. J. Wiley, *Nanoscale*, 2014, **6**, 5980-5988.
44. Y. G. Sun, B. Mayers, T. Herricks and Y. N. Xia, *Nano Lett.*, 2003, **3**, 955-960.
45. Z. Jiang, Y. Tian and S. Ding, *Mater. Lett.*, 2014, **136**, 310-313.
46. C. J. Johnson, E. Dujardin, S. A. Davis, C. J. Murphy and S. Mann, *J. Mater. Chem.*, 2002, **12**, 1765-1770.
47. N. Murshid and V. Kitaev, *Chem. Commun.*, 2014, **50**, 1247-1249.

48. H. J. Yang, S. Y. He and H. Y. Tuan, *Langmuir*, 2014, **30**, 602-610.
49. A. R. Rathmell and B. J. Wiley, *Adv. Mater.*, 2011, **23**, 4798-4803.
50. T. C. Hauger, S. M. I. Al-Rafia and J. M. Buriak, *ACS Appl. Mater. Interfaces*, 2013, **5**, 12663-12671.
51. D. S. Leem, A. Edwards, M. Faist, J. Nelson, D. D. C. Bradley and J. C. de Mello, *Adv. Mater.*, 2011, **23**, 4371-4375.
52. X. Y. Zeng, Q. K. Zhang, R. M. Yu and C. Z. Lu, *Adv. Mater.*, 2010, **22**, 4484-4488.
53. H. Z. Guo, N. Lin, Y. Z. Chen, Z. W. Wang, Q. S. Xie, T. C. Zheng, N. Gao, S. P. Li, J. Y. Kang, D. J. Cai and D. L. Peng, *Sci Rep-Uk*, 2013, **3**.
54. A. R. Rathmell, M. Nguyen, M. F. Chi and B. J. Wiley, *Nano Lett.*, 2012, **12**, 3193-3199.
55. J. Z. Song, J. H. Li, J. Y. Xu and H. B. Zeng, *Nano Lett.*, 2014, **14**, 6298-6305.
56. J. Z. Song and H. B. Zeng, *Angew Chem Int Edit*, 2015, **54**, 9760-9774.
57. Y. Cheng, S. L. Wang, R. R. Wang, J. Sun and L. Gao, *J. Mater. Chem. A*, 2014, **2**, 5309-5316.
58. E. C. Garnett, W. S. Cai, J. J. Cha, F. Mahmood, S. T. Connor, M. G. Christoforo, Y. Cui, M. D. McGehee and M. L. Brongersma, *Nat. Mater.*, 2012, **11**, 241-249.
59. S. Han, S. Hong, J. Ham, J. Yeo, J. Lee, B. Kang, P. Lee, J. Kwon, S. S. Lee, M. Y. Yang and S. H. Ko, *Adv. Mater.*, 2014, **26**, 5808-5814.
60. P. Lee, J. Lee, H. Lee, J. Yeo, S. Hong, K. H. Nam, D. Lee, S. S. Lee and S. H. Ko, *Adv. Mater.*, 2012, **24**, 3326-3332.

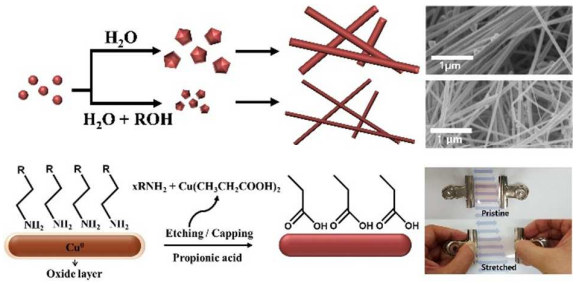

The stretchable transparent electrode was achieved with the rationally controlled ultra-long copper nanowire and the low temperature direct spray coating.